https://dx.doi.org/10.22161/ijaers.5.12.32 ISSN: 2349-6495(P) | 2456-1908(O)

Development of a Wireless Data Acquisition System for Application in Real-Time Closed-Loop Control Systems

Lillyane R. Cintra[1], Matheus F. Mollon[2], Eduardo H. Kaneko[3],Marcio A. F. Montezuma[4],Márcio Mendonça[5]

[1,2,3]Graduate Student, University of Technology - Paraná, CornélioProcópio, Paraná, Brazil
Email: lillyanecintra@alunos.utfpr.edu.br[1],matheusmollon@alunos.utfpr.edu.br[2], eduardok@alunos.utfpr.edu.br[3]
[4]Department of Mechanical Engineering, University of Technology - Paraná, CornélioProcópio, Paraná, Brazil
Email: montezuma@utfpr.edu.br[4]
[5]Department of Electrical Engineering, University of Technology - Paraná, CornélioProcópio, Paraná, Brazil
Email:mendonca@utfpr.edu.br[5]

Abstract*—This paper presents the development of a wireless data acquisition system (WDAS) of incremental encoder sensors, for application in the real-time closed-loop control systems.The wireless technologies evaluated for the system were 433 MHz radio frequency (RF) and Bluetooth 2.0. The developed system was applied to the angular velocity control of a permanent magnet direct current (PMDC) motor, as a way of evaluating its development and also the time of communication with the different wireless technologies. The WDAS with the 433 MHz RF wireless module presented a satisfactory result, while the WDAS with the Bluetooth 2.0 wireless module was not adequate to this real-timeclosed-loop control system.*

Keywords*—*Wireless Data Acquisition, Real-Time, Control Systems.

I. INTRODUCTION

A fundamental part in the development of control systems is the data acquisition system, which allows the acquisition of information from a plant through the reading of sensors [1].The conventional way of operating these systems is by means of the wired monitoring of the plant, due to its reliability in data transmission [2].However, there are systems where wired acquisition is inconvenient, e.g. in a modified Ball and Beam [3] and in photovoltaic systems [2].In the first, the wired acquisition of the cart position causes the limitation of its movement [3]. In the second, the use of cables increases the cost of installation and maintenance [2].

Acquisition systems applied in control have the desired characteristic of operating in real-time, being essential in critical control applications [1, 4].In the case of wireless data acquisition systems (WDAS), the time delay between sampling and application of the control signal, as a resultof the data transmission time, may limit the sampling rate of the system.In addition, time delays in reading sensors can lead to system instability and poor control performance, when not taken into account in the controller design [4].

In this context, the work develops a hardware and firmware fora WDAS of a position sensor, i.e. a wireless sensor, the structure of which is typically composed of a sensor, a processing unit, memory and a wireless radio [4].The processing unit used was the microcontroller PIC18F2331, which has enough memory for the developed application.The position sensor is a quadrature encoder type, which is read using the quadrature encoder interface (QEI) of the PIC18F2331 microcontroller.The technologies of the wireless radios used are 433 MHz radio frequency (RF) and Bluetooth 2.0, respectively, the Canton-Electronics'HYTRP-RS232 and DFRobot'sDF-BluetoothV3.

The purpose of the developed system is the application in real-timeclosed-loop control systems, therefore its performance was evaluated in the angular velocity control of a permanent magnetic direct current (PMDC)motor, through wired, radio frequency and Bluetooth 2.0 data acquisition.The paper is organized as follows. Section II presents related works. In Section III it is presented the methodology and the materials used in the system development. Section IV presents the validation of the WDAS. Section V presents the obtained results. Section VI presents the conclusions of the study.

II. RELATED WORK

The work [4] presents the development of a real-time wireless data acquisition board and its software, for

https://dx.doi.org/10.22161/ijaers.5.12.32 *ISSN: 2349-6495(P) | 2456-1908(O)*

application in the monitoring of structural health in civil engineering.The work is focused on the study of the latency introduced in the control loop by the data acquisition hardware, a low latency hardware solution was developed.

In the work [5], an architecture for the wireless data acquisition applied in the continuous monitoring of ambient radioactivity is presented.Since this monitoring occurs in large, inaccessible and risky areas, the use of wireless sensors is interesting, but the energy consumption of the equipment represents a limitation in its use.The objective of the work was to develop an accurate acquisition system, with self-sustainability and efficiency in energy consumption.

The work [6] proposes an intelligent wireless sensor, which uses the Arduino platform, able to acquire in real time the transverse displacement of railroadbridges under workload.The objective of the work is that the proposed platform is efficient and low cost.The authors validated the platform in the laboratory proving that the system is able to acquire the transverse displacement and transmit it in real-time wirelessly.

In the work [7], an industrial synchronous wireless data acquisition system using the IEEE 802.11n protocol to implement a high-speed transmissionis presented.The purpose of the work was to develop a solution capable of synchronously acquiring the data and allowing the transmission of a larger amount of data with limited bandwidth.Through experiments, the authors concluded that the system can be used in synchronous data acquisition and real-time analysis for applications such as power electronics analysis and bridge health monitoring.

III. DEVELOPMENT

This section elucidates the materials and methodology applied in the development of the system.

3.1 Wireless Data Acquisition System Overview

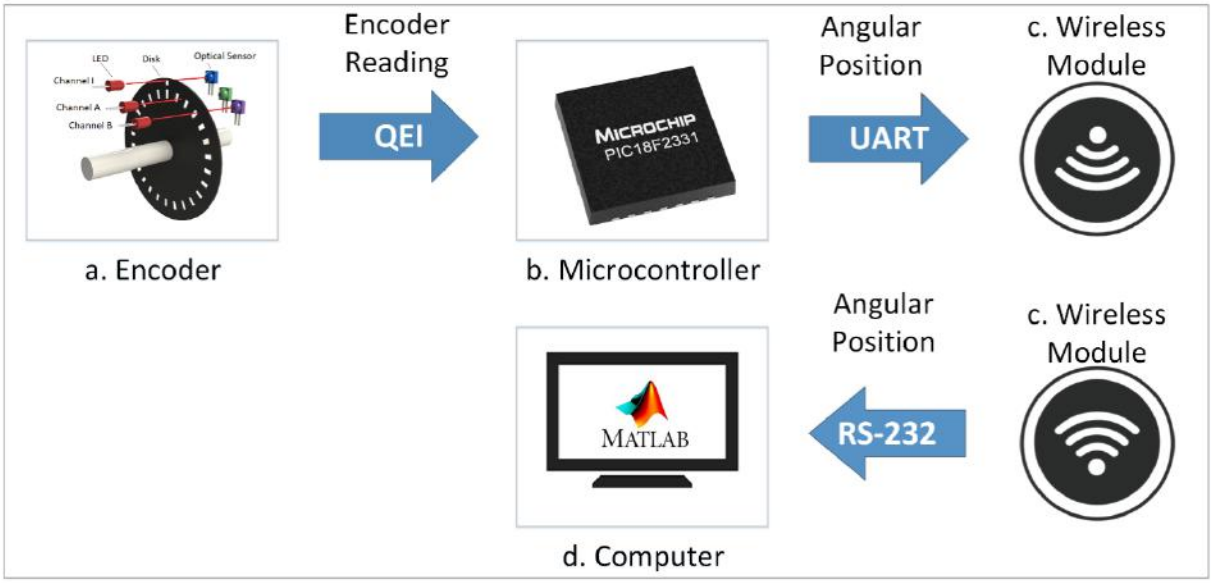

Fig.1: Wireless data acquisition system overview.

Fig. 1 presents the overview of the developed WDAS for reading the position of a quadrature encoder.The processing unit is Microchip's PIC18F2331 microcontroller (Fig. 1b), responsible to read the encoder position, through the QEI module, and send this information through the UART serial communication to the module (Fig. 1c) responsible for the wireless transmission.The other module performs the wireless reception of the encoder position, and transmits to the interface developed in MATLAB/Simulink (Fig. 1d) via RS232 communication.

The wireless modules used in this project weretwo Canton-Eletronics' HYTRP-RS232 and twoDFRobot's DF-BluetoothV3, both configured with a baud rate of 57,600 bits per second (bps), for communication with the microcontroller (Fig. 1b) and the computer (Fig. 1d).In this scenario, the wireless modules were evaluated, in relation to the total data transmission time, in order to verify the best technology for data acquisition in real-time. Section V presents the results that aided in the choice of the wireless technology for the WDAS.

3.2 Development of the Wireless Data Acquisition Hardware

The WDAS for encoder reading was made on a printed circuit board (PCB) comprising connectors for any type of incremental encoder of 5V or 3.3V, in addition to the microcontroller PIC18F2331 and a connector for the wireless module.

https://dx.doi.org/10.22161/ijaers.5.12.32 *ISSN: 2349-6495(P) | 2456-1908(O)*

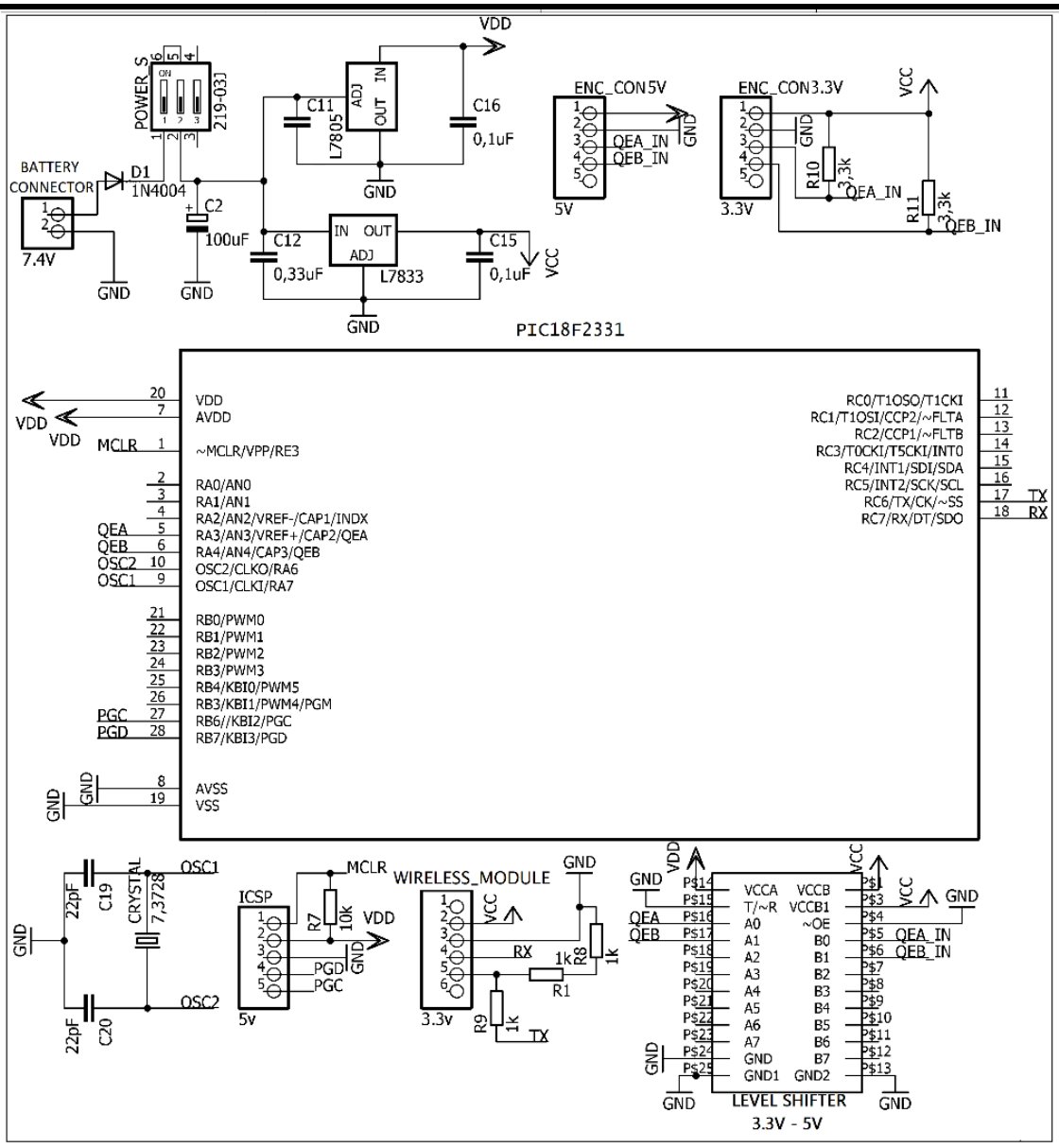

Fig.2: Presents the complete schematic of the PCB.

3.3 Development of the Wireless Data Acquisition Firmware

The firmware, built in C language, embedded in the microcontroller has its execution flow described in Fig. 3.In general, the peripherals and interruptions settings step configures the microcontroller's QEI module for X4 encoding and free counting mode, wherein the counter is automatically reset when the maximum count value is reached.In addition to configuring the UART transmission module with a baud rate of 57,600 bps.

The system works with requests initiated by sending the specific command of the implemented functionality.The waiting for the requests, through the serial read interrupt, occurs in step 2 of Fig. 3.If the received command matches the “request sample” command, the system reads the 32-bit encoder count variable and sends it within a response protocol to the computer via wireless transmission. After sending, the system returns to step 2.

The systemhas only one response protocol that contains a header byte (HB), the encoder reading data bytes(DB), and an end of transmission byte (EB). Table 1 shows the bytes that make up the HB and EB, besides the commands of the implemented functionalities.

Table 1: Commands and protocol bytes used in serial communication.

Byte (Decimal)	Description
40	Protocol Header Byte
41	End of Transmission Byte
123	Request Sample Command
67	Reset Encoder Counting Command

https://dx.doi.org/10.22161/ijaers.5.12.32 ISSN: 2349-6495(P) | 2456-1908(O)

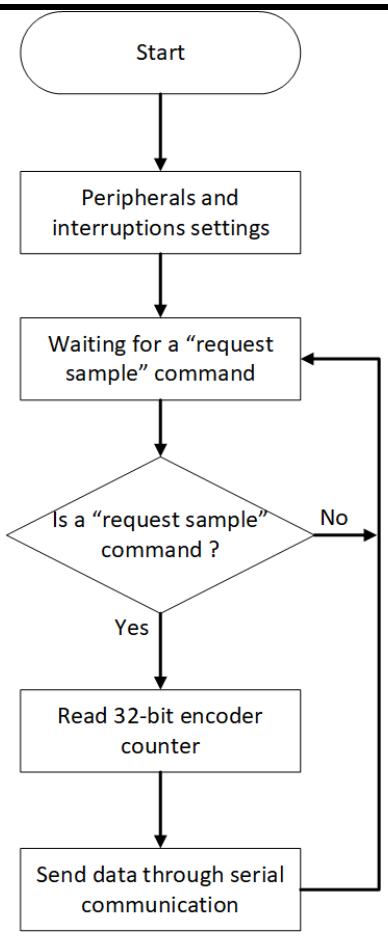

Fig.3: Firmware flowchart.

3.4 Development of the MATLAB/Simulink Interface

The interface for sending the commands and acquiring the encoder position can be developed in any program or programming language capable of manipulating the serial ports of the computer. However, since the objective is to use the WDAS in real-time closed-loop control systems, the interface was developed in MATLAB/Simulink 2012a software.

To do so, the Real-Time Windows Target toolbox was used, which provides a kernel for running real-time models in the Windows operating system [8]. In addition to presenting libraries for handling Input/Output (I/O) devices of the computer, e.g. the serial ports [8].

Fig. 4 illustrates the Simulink block diagram for reading the encoder position through the developed WDAS.The diagram shows the sending of the "request sample" command and the reception of the response protocol with the encoder position, which is converted to angular position in radians (rad).The Simulink block diagram model operates in discrete mode with fixed fundamental sample time (Δt). When executing the interface, at each Δt is sent the request command and received the response protocol.

The encoder position is a 32-bit variable whose count ranges from 0 to 4,294,967,295. The relation in (1) converts the encoder position to angular position (rad).

$$R = \frac{C \ 2\pi}{X \ PPR} \quad \ldots\ldots\ldots\

https://dx.doi.org/10.22161/ijaers.5.12.32 *ISSN: 2349-6495(P) | 2456-1908(O)*

IV. VALIDATION OF THE WIRELESS DATA ACQUISITION SYSTEM

The validation of theWDAS for reading the encoder position was made through the angular velocitycontrol of the PMDC motor F2140 from Maxon. The linear state-space model of the PMDC motor was extracted from [9]. Its representation is given in (2) and (3).

$$\frac{d}{dt}\begin{bmatrix}\omega_m \\ I_a\end{bmatrix} = \begin{bmatrix}-b/J & K_t/J \\ -K_e/L_a & -R_a/L_a\end{bmatrix}\begin{bmatrix}\omega_m \\ I_a\end{bmatrix} + \begin{bmatrix}0 \\ 1/L_a\end{bmatrix}V_a \quad ..(2)$$

$$y = \begin{bmatrix}1 & 0\end{bmatrix}\begin{bmatrix}\omega_m \\ I_a\end{bmatrix} \quad .....(3)$$

Table 2 describes the parameters in (2) and (3) and presents their respective values identified in the work [10].

Table 2: PMDC motor parameters.

Parameter	Units	Description
$b = 2.33x10^{-6}$	$\frac{Nm.s}{rad}$	Viscous Friction Constant
$J = 2.32x10^{-6}$	$Kg.m^2$	Moment of Inertia
$K_e = 0.027439$	$\frac{V.s}{rad}$	Electromotive Force Constant
$K_t = 0.027439$	$\frac{Nm}{A}$	Motor Torque Constant
$L_a = 0.0015168$	H	Armature Inductance
$R_a = 10.223$	Ω	Armature Resistance
V_a	V	Supply Voltage
I_a	A	Direct Current
ω_m	$\frac{rad}{s}$	Angular Velocity

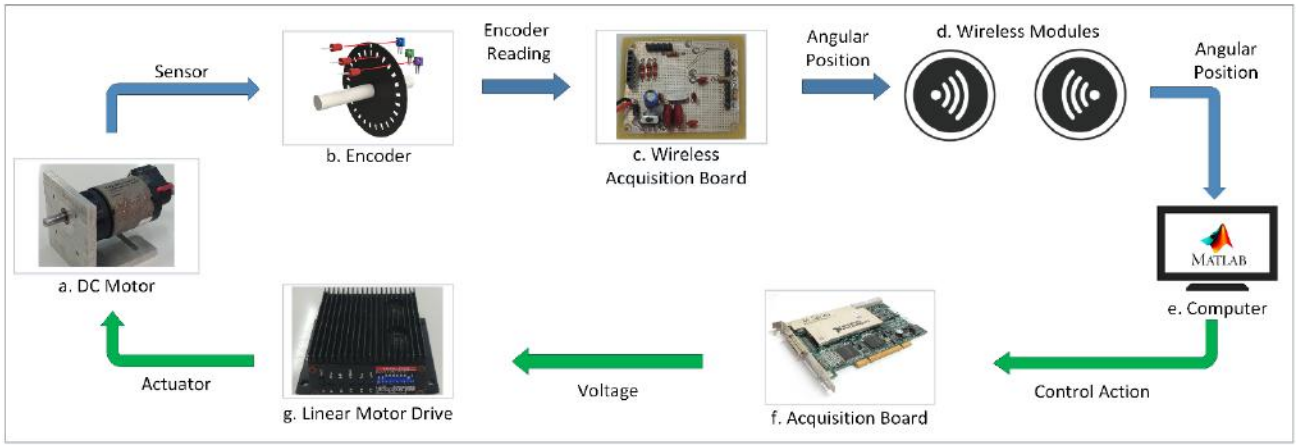

Fig. 5: PMDC motor angular velocity control system.

Fig. 5 shows the angular velocity control system of the F2140 motor (Fig. 5a), which has a quadrature encoder (Fig. 5b), with a resolution of 100 pulses per revolution, coupled to its shaft. The WDAS, which comprises the components in Fig. 5c and Fig. 5d, performs the reading and wireless transmission of the encoder position to the computer (Fig. 5e). In this was developed the real-time closed-loop control.

The angular velocity control of the motor was made in the MATLAB/Simulink. From the encoder position, received via WDAS, the angular velocity (rad/s) is calculated. This is used to obtain the error applied to the controller to determine the control action in Volts (V).The National Instruments PCI-6251 acquisition board (Fig. 5f) applies the control action on the Maxon LSC 30-2 linear drive (Fig.5g) which actuates the F2140 motor in its voltage operation range, closing the control loop.

The controller implemented to stabilize the motor angular velocity is the PID controller. According to [11], this type of controller is composed of three terms: Proportional, Integral and Derivative. Each of them performs mathematical operations on the error function $e(t)$, the sum of these operations results in the control action $u(t)$ applied to the system.In (4) is denoted the content of the error function.

$$e(t) = r(t) - y(t) \quad .....(4)$$

where$r(t)$ is the reference angular velocity and $y(t)$ is the angular velocity response of the PMDC motor. In (5) is presented the PID control law.

$$u(t) = K_p\, e(t) + K_i \int_0^t e(t)\, dt + K_d \frac{de(t)}{dt} \quad .....(5)$$

Where K_p, $K_i$and$K_d$are the proportional, integral and derivative gains, respectively.

https://dx.doi.org/10.22161/ijaers.5.12.32 *ISSN: 2349-6495(P) | 2456-1908(O)*

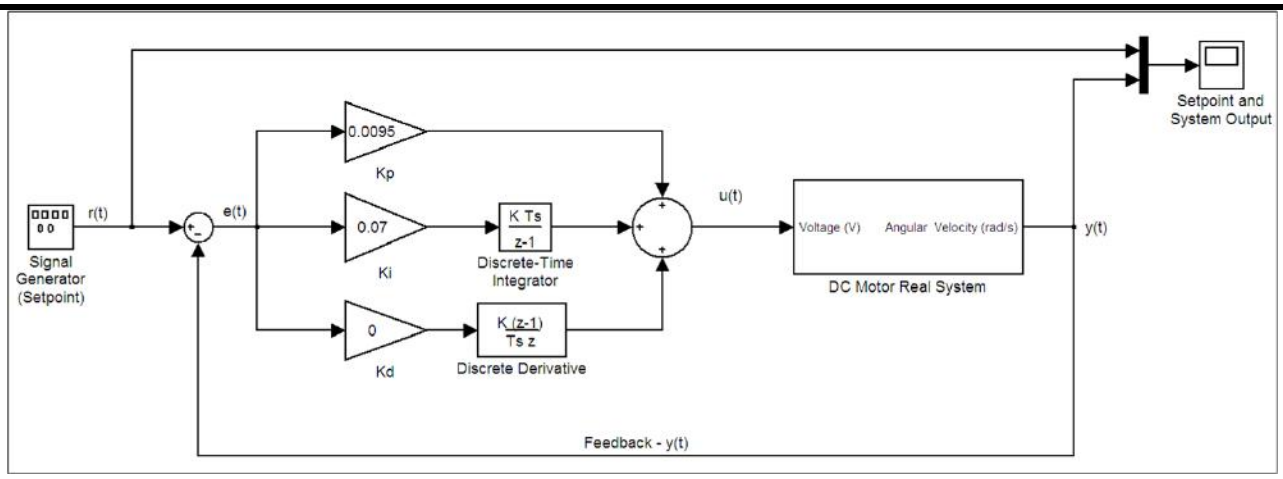

Fig. 6: DC motor angular velocity controller in MATLAB/Simulink.

Based on the state-space model of the motor in (2) and (3), in the motor parameters in Table 2 and in the control law in (5), the real-time closed-loop control was built in the MATLAB/Simulink software, as shown in Fig. 6.

The block diagram in Fig. 6 is discretized for its application in the realPMDC motor control system. In this context, the integral and derivative terms of the control law are calculated numerically as indicated in the Fig. 6.The diagram shows a subsystem that indicates the PMDC motor to be controlled, which is explained in Fig. 7.

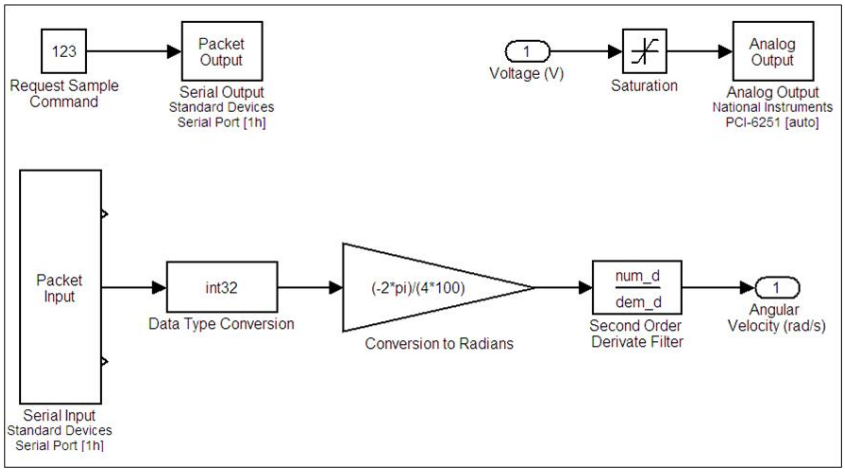

Fig. 7: DC motor subsystem block in MATLAB/Simulink.

In Fig. 7, the voltage (V) applied to the motor drive is limited by a saturator in the range of - 10V to 10V, that is the range on which the PCI-6251 analog output works. In addition, to achieve the operating voltage of the 12V motor, an internal gain was set in the linear drive. The negative voltage present in the operating range is applied to the motor to reverse its direction of rotation.

With respect to the calculation of the angular velocity (rad/s), the position of the encoder is converted to angular position (rad), according to (1), and after, with the aid of a second-order derivative filter, is converted to angular velocity (rad/s).In (6), the transfer function of the second order derivative filter is illustrated.

$$TF = \frac{{\omega_{cf}}^2 s}{s^2 + 2\zeta\,\omega_{cf}\, s + {\omega_{cf}}^2} \quad \ldots\ldots\ldots\ldots\ldots\ldots\ldots\ldots (6)$$

where$\zeta$is the filter damping ratio and $\omega_{cf}$is the filter cutting frequency, defined in (7).

$$\omega_{cf} = 2\pi f \quad \ldots\ldots\ldots\ldots\ldots\ldots\ldots\ldots\ldots\ldots\ldots\ldots (7)$$

where$f$is the cut-off frequency in Hertz (Hz).

V. RESULTS

The real-time closed-loop control of the PMDC motor angular velocity was evaluated for the wired data acquisition and for the WDAS, with the RF and Bluetooth 2.0 modules. For this, the response of the real control for all forms of acquisition was compared to the response of the simulated control by the model in (2) and (3). In addition, the communication time of all forms of acquisition was evaluated. Table 3 presents the PID controller gains, damping ratio and cutting frequency of the derivative filter, all obtained empirically.

The comparison of real and simulated control responses are shown in Figs. 8 and 9. Fig. 8 shows the control for a square wave set point and Fig. 9 for a sinusoidal

https://dx.doi.org/10.22161/ijaers.5.12.32 *ISSN: 2349-6495(P) | 2456-1908(O)*

wavesetpoint, both with amplitude of 200 rad/s and frequency of 0.1 Hz.

Table 3: General settings.

Parameter	Value	Description
K_p	0.0095	Proportional Gain
K_i	0.07	Integral Gain
K_d	0.0	Derivative Gain
ζ	1.6	Filter Damping Ratio
f	15 Hz	Filter Cutting Frequency
Δt	0.02s	Sample Time

In Figs. 8 and 9, dashed lines in blue illustrate the set point. The solid line in red indicates the control response of the simulated model. The solid lines in green, pink and black colors indicate the real motor control responses for WDAS with Bluetooth 2.0, wired, and WDAS with RF acquisitions, respectively.

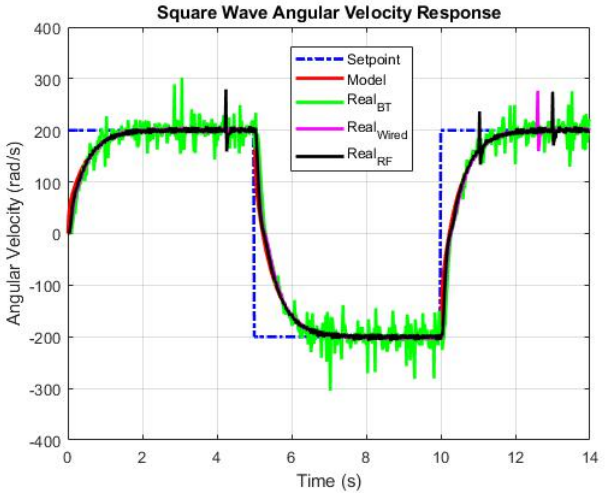

Fig. 8: PMDC motor angular velocity control response (square wave).

Fig. 8 shows that the system reaches the desired setpoint around two seconds for all motor control responses. In addition, the real control responses are in accordance to the simulated control response.This can be verified through the Normalized Root Mean Square Error (NRMSE), in Table 4, which evaluates how accurateis the fit between the response of the real controls and the response of the simulated control.

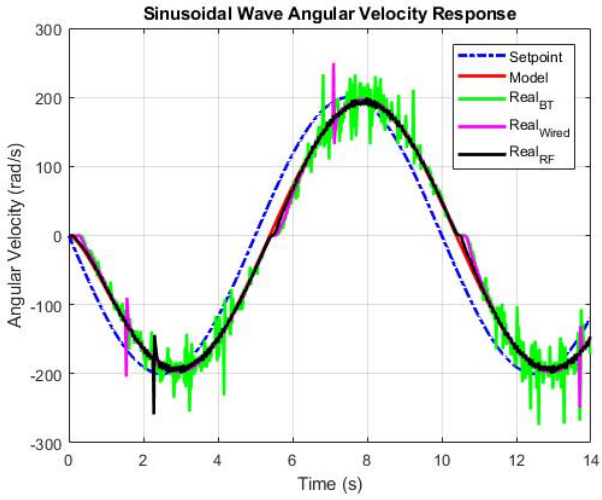

Fig. 9: PMDC motor angular velocity control response (sinusoidal wave).

As seen in Fig. 9, the real control responses are in accordance with the simulated control response. In addition to maintaining the characteristics of the setpoint, even with a delay around 0.4s. Table 4 presents the NRMSE calculation for the control responses with the square and sinusoidal wave set point. A result of 100% indicates that the responses are identical.

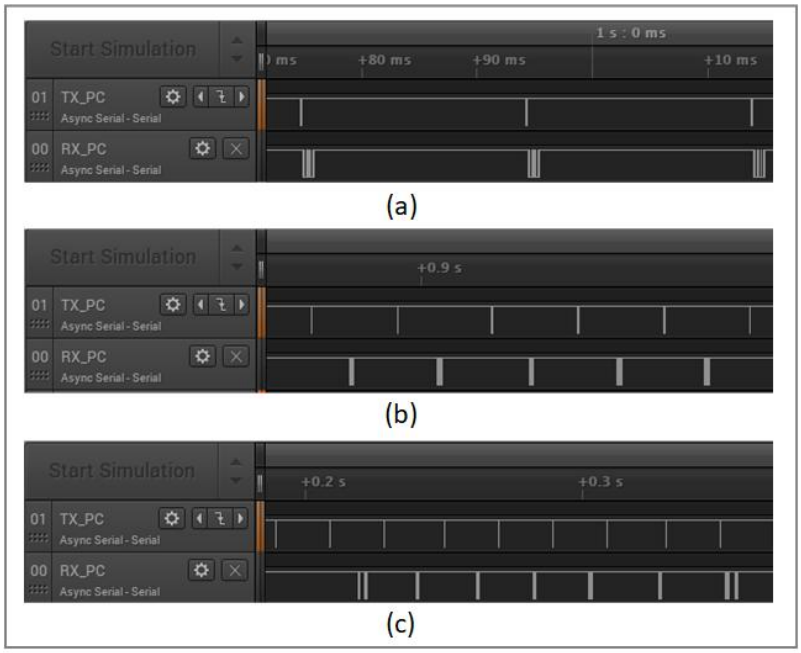

Fig. 10: Serial transmission/reception responses: (a) Wired; (b) Radio frenquency; (c) Bluetooth 2.0.

https://dx.doi.org/10.22161/ijaers.5.12.32 *ISSN: 2349-6495(P) | 2456-1908(O)*

Table 4: NRMSE between the simulated control response and the real control responses, for all modes of acquisition.

Wave	NRMSE Wired (%)	NRMSE Radio Frequency (%)	NRMSE Bluetooth (%)
Square	91.75	92.57	83.70
Sinusoidal	92.95	95.89	85.98

The evaluation of the communication time was performed using the Logic Pro 16 logic analyzer from Saleae. This, connected to the serial port of the computer, observes the sending of the command "request sample" and the reception of the response protocol. Respectively, through the transmission (TX) and receive (RX) channels of the computer serial port. The communication time is calculated in (8).

$$t_C = t_{ERP} - t_{IRST} \quad (8)$$

where t_C is the communication time, t_{ERP} is the time at the end of the response protocol reception and t_{IRST} is the initial time of the command "request sample" transmission.

Fig. 10 illustrates part of the data transmission/reception between the computer and all forms of acquisition, respectively, the wired communication (Fig. 10a), the WDAS with the RF modules (Fig. 10b) and the WDAS with the Bluetooth 2.0 modules (Fig. 10c).

Table 5 shows the average communication time for all forms of acquisition, considering 180 samples. In addition to the standard deviation with 95% confidence interval, according to the student'st-distribution.

Table 5: Data acquisition communication time.

Data Acquisition	Sample delay Time (ms)
Wired	1.2418 ± 0.0100
WDAS + Radio Frequency	10.1279 ± 0.7728
WDAS + Bluetooth 2.0	41.3627 ± 17.3689

VI. CONCLUSIONS

This work presented the development of a WDAS of encoder type sensors, for the application in real-time closed-loop control of systems. For this, its performance was evaluated in the angular velocity control of a PMDC motor, for the wired, radio frequency and Bluetooth 2.0 data transmission.In addition, the communication time of the wireless transmission modules was studiedto define the best technology to be incorporated into the WDAS.

In the PMDC motor control for square and sinusoidal setpoint signals, the responses obtained by the wired acquisition and WDAS, with RF and Bluetooth 2.0, followed the behavior of the simulated control, as shown in Figs. 8 and 9.However, it is possible to note the presence of noise in the response signals. This can occur due to the low resolution of the encoder attached to the motor, which is 100 pulses per revolution. All the signals may eventually present some noise, such as the response signal from the wired acquisition and the WDAS with RF.However, the noise present in the entire response signal of the WDAS with Bluetooth 2.0 is also due to the operating characteristic of the wireless module.

In the analysis of the communication time of the data acquisition, it was possible to estimate the time to acquire the position of the encoder. In the context of real-time closed-loop control, it is necessary that the communication time is shorter than the sampling time, in addition to presenting small variation, so that one can consider that there is a determinism of time in the data acquisition.

As shown in Table 5, the RF was the best wireless technology evaluated, since the communication time was shorter than the sampling time used, in this case of 20 ms, besides presenting a standard deviation of less than 1 ms, for the confidence interval of95%.In the case of Bluetooth 2.0, the communication time was more than two times greater than the sampling time, besides presenting a standard deviation slightly less than the sampling time.Therefore, the delay and variation of time in the acquisition of the encoder position with the Bluetooth 2.0 module, led to a control signal noisier than that of the other forms of acquisition, as shown in Figs. 8 and 9.

Finally, the results obtained in this work are valid only for the Canton-Electronics' HYTRP-RS232 and the DFRobot's DF-BluetoothV3 modules, in addition to considering transmission of one byte and the reception of six bytes. If this set changes, the response times will also change and a new study of the communication time will be necessary.

REFERENCES

[1] S. Bao, H. Yan, Q. Chi, Z. Pang and Y. Sun, FPGA-Based reconfigurable data acquisition system for industrial sensors, in IEEE Transactions on Industrial Informatics, vol. 13, no. 4, pp. 1503-1512, 2017.

[2] F. Shariff, N. A. Rahim, W. P. Hew, Zigbee-based data acquisition system for online monitoring of grid-connected photovoltaic system, in Expert Systems with Applications, vol. 42, no. 3, pp. 1730-1742, 2015.

[3] L. Niro, E. H. Kaneko, M. F. Mollon, W. de S. Chaves, M. A. F. Montezuma. Control of a modified ball and beam system using tracking system in real time with a dc motor as an actuator, in International Journal of Advanced Engineering Research and Science, vol.4, no. 12, pp. 099-107, 2017.

https://dx.doi.org/10.22161/ijaers.5.12.32 ISSN: 2349-6495(P) | 2456-1908(O)

[4] L. E. Linderman, H. Jo and B. F. Spencer, Low-latency data acquisition hardware for real-time wireless sensor applications, in IEEE Sensors Journal, vol. 15, no. 3, pp. 1800-1809, 2015.

[5] A. Gomez, M. Magno, M. F. Lagadec and L. Benini, Precise, energy-efficient data acquisition architecture for monitoring radioactivity using self-sustainable wireless sensor nodes, in IEEE Sensors Journal, vol. 18, no. 1, pp. 459-469, 2018.

[6] A.I. Ozdagli, B. Liu, F. Moreu, Low-cost, efficient wireless intelligent sensors (LEWIS) measuring real-time reference-free dynamic displacements, in Mechanical Systems and Signal Processing, vol. 107, pp. 343-356, 2018.

[7] Y. Yuan, Q. Xu, X. Guan, Z. Liu, Industrial high-speed wireless synchronous data acquisition system with real-time data compression, in Measurement, vol. 46, no. 9, pp. 3482-3487, 2013.

[8] MathWorks, Real-Time Windows Target: User's Guide, 2nd ed., The MathWorksInc, 2000.

[9] J. D'azzo; C. Houpis. Linear control system analysis and design: conventional and modern. 4th ed. New York: McGraw-Hill Companies, 1995.

[10] W. de S. Chaves, E. H. Kaneko, M. F. Mollon, L. Niro, A. do N. Vargas, M. A. F. Montezuma. Parameters Identification of a Direct Current Motor Using the Trust Region Algorithm, in International Journal of Advanced Engineering Research and Science,vol.4,no. 12, pp.162-169,2017.

[11] K.J. Aström andT. Hägglund, PID controllers: theory, design and tuning, 2nded., Instrument Society of America, NC, USA, 1995.